HHS Public Access

Author manuscript

J Alzheimers Dis. Author manuscript; available in PMC 2019 November 11.

Published in final edited form as:

J Alzheimers Dis. 2019 ; 71(3): 979–991. doi:10.3233/JAD-190604.

Quantification of tau protein lysine methylation in aging and Alzheimer's disease

Carol J. Huseby[a,1], **Claire N. Hoffman**[b,1], **Grace L. Cooper**[b], **Jean-Christophe Cocuron**[c], **Ana P. Alonso**[c], **Stefani N. Thomas**[d], **Austin J. Yang**[d], **Jeff Kuret**[a,b,e,*]

[a]Interdisciplinary Biophysics Graduate Program, Ohio State University, Columbus, OH, USA

[b]Ohio State Biochemistry Program, Ohio State University, Columbus, OH, USA

[c]BioDiscovery Institute, University of North Texas, Denton, TX, USA

[d]Department of Anatomy and Neurobiology; Molecular & Structural Biology Program, Greenebaum Cancer Center, University of Maryland, Baltimore, MD, USA

[e]Department of Biological Chemistry & Pharmacology, Ohio State University, Columbus, OH, USA

Abstract

Tau is a microtubule-associated protein that normally interacts in monomeric form with the neuronal cytoskeleton. In Alzheimer's disease, however, it aggregates to form the structural component of neurofibrillary lesions. The transformation is controlled in part by age- and disease-associated post-translational modifications. Recently we reported that tau isolated from cognitively normal human brain was methylated on lysine residues, and that high-stoichiometry methylation depressed tau aggregation propensity *in vitro*. However, whether methylation stoichiometry reached levels needed to influence aggregation propensity in human brain was unknown. Here we address this problem using liquid chromatography–tandem mass spectrometry approaches and human-derived tau samples. Results revealed that lysine methylation was present in soluble tau isolated from cognitively normal elderly cases at multiple sites that only partially overlapped with the distributions reported for cognitively normal middle aged and AD cohorts, and that the quality of methylation shifted from predominantly dimethyl-lysine to monomethyl-lysine with aging and disease. However, bulk mol methylation/mol tau stoichiometries never exceeded 1 mol methyl group/mol tau protein. We conclude that lysine methylation is a physiological post-translational modification of tau protein that changes qualitatively with aging and disease, and that pharmacological elevation of tau methylation may provide a means for protecting against pathological tau aggregation.

[*]Correspondence to: Jeff Kuret, PhD, Department of Biological Chemistry & Pharmacology, Ohio State University, 1060 Carmack Rd, Columbus, Ohio, 43210, USA. *Tel:* 614-688-5899, kuret.3@osu.edu.

[1]Equal contribution

Conflict of Interest/Disclosure

The authors have no conflict of interest to report

Keywords

Alzheimer's disease; tau protein; post-translational modification; phosphorylation; methylation; mass spectrometry; aging

Introduction

Alzheimer's disease (AD) is defined in part by the appearance of neurofibrillary lesions in the neocortex and other brain regions (reviewed in [1, 2]). The lesions accumulate aggregated forms of tau, a microtubule-associated protein that normally functions in human brain as an ensemble of six monomeric isoforms to stabilize microtubules and promote their assembly (reviewed in [3]). The conversion of tau into aggregated forms correlates with cognitive decline [4], and potentially serves as a vector for spreading tau misfolding across brain regions [5, 6]. The pathways through which tau aggregates in disease are not fully characterized but may be initiated and controlled through post-translational modifications (PTMs). For example, Ser/Thr phosphorylation modulates tau/microtubule affinity [7, 8], thereby controlling concentrations of free tau on which aggregation rate depends [9]. Phosphorylation also can directly increase tau aggregation propensity [10, 11]. The phosphorylation sites occupied in normal and disease states overlap substantially but incompletely (reviewed in [12, 13]), indicating that the qualitative location of phosphorylation sites may influence tau function in disease. Yet the most compelling case for involvement of this modification comes from quantification of its stoichiometry, which increases from 2–3 mol phosphate/mol tau protein in post-mortem samples of cognitively normal brain to 89 mol/mol in AD brain (reviewed in [14]). It is these quantitative as well as qualitative differences that characterize "tau hyperphosphorylation" in AD, and support its proposed function as a gatekeeper for entry into aggregation pathways [14].

Tau also is modified on Lys residues by ubiquitylation and acetylation, and these too are candidate modifications for influencing tau lesion formation (reviewed in [15]). Because ubiquitylation is transient and linked to tau clearance [16, 17], its effects on tau aggregation rate are likely exerted indirectly through control of bulk tau levels. In contrast, Lys acetylation can raise tau aggregation propensity in biological models [18, 19]. Tau acetylation has been detected in human brain primarily using highly sensitive immunological reagents raised against specific sites [19–21], and two of these (AcK174 and AcK280) have been confirmed using proteomic methods [19, 22]. Although relative tau acetylation occupancy increases with disease progression in neocortex [19, 23], absolute stoichiometries have not been reported for any human cohort.

Using proteomic methods, we recently showed that brain-derived human tau protein was methylated at multiple Lys residues, some of which overlapped with reported acetylation and ubiquitylation sites [24, 25]. Moreover, tau isolated from cognitively normal middle age and AD cohorts differed in methyl Lys site distributions [24, 25]. Uniquely among Lys modifications, however, high-stoichiometry methylation (*i.e.*, ~5 mol methyl groups/mol tau protein) depressed aggregation propensity of tau *in vitro* without inhibiting its microtubule assembly promoting activity [24]. These findings suggest that Lys methylation could be a

mechanism for restraining tau aggregation propensity if sufficient site occupancy were attained. However, as with other Lys modifications, the stoichiometry of tau methylation in human brain is unknown.

Here we extend mass spectrometry-based detection of tau PTMs to a human cohort composed of cognitively normal elderly individuals with two objectives in mind. First, through comparison with the previously reported methyl-Lys site distribution in cognitively normal middle-aged individuals [24], we examine whether tau methylation sites change with aging in cognitively normal individuals. A positive result could identify a potential age-related driver of tau lesion formation, and a biomarker for aggregation risk. Second, we test whether bulk occupancy of methylation sites changes in soluble tau with aging and with aggregation in disease. The results show that Lys methylation is detectable in all examined human cohorts, and that it changes qualitatively with aging and disease, but that its stoichiometry remains low (≤1 mol methyl group/mol tau protein) relative to phosphorylation in both soluble and aggregated tau preparations.

Materials and Methods

Human brain-derived soluble tau protein

Archival, de-identified postmortem human brain tissue from autopsies performed with informed consent of each patient or relative was used for tau purification. Soluble brain-derived tau was enriched using methods detailed previously [26]. All purification steps and centrifugations were carried out at 4°C unless stated otherwise. Gray matter from neocortical regions (Table 1) was homogenized (Teflon-glass homogenizer operated ten strokes at 1000 RPM) in 5 volumes of homogenization buffer (20 mM MES, pH 6.8, 80 mM NaCl, 1 mM $MgCl_2$, 2 mM EGTA, 0.1 mM EDTA, 1 mM PMSF) containing inhibitors of phosphoprotein phosphatases (10 mM sodium pyrophosphate, 20 mM NaF, 1 mM Na_3VO_4) and deacetylases (2 μM trichostatin A, 10 mM nicotinamide). After centrifugation (27,000 × *g*, 20 min), the supernatant was collected, adjusted to 0.5 M NaCl and 2% 2-mercaptoethanol, boiled for 10 min, and recentrifuged (27,000 × *g*, 20 min). The resulting heat-stable supernatant fraction was treated with 2.5% perchloric acid (final concentration). After isolating the acid-soluble fraction by centrifugation (27,000 × *g*, 20 min), protein was concentrated by 20% (w/v) trichloroacetic acid (TCA) precipitation followed by two washes in cold acetone. Dry protein pellets were stored at −20°C until used.

Human brain-derived tau filaments (PHF-tau)

Authentic human tau filaments were purified from AD cases using a modification of two procedures [27, 28]. Gray matter from neocortical regions (Table 1) was minced and homogenized with a blender in five volumes of homogenization buffer containing phosphoprotein phosphatase and deacetylase inhibitors. The mixture was further homogenized in a Teflon-glass homogenizer (ten strokes at 1000 RPM) and centrifuged (27,000 × *g*, 20 min). After discarding the supernatant, the pellet was resuspended in 10 volumes of 0.8 M NaCl, 10% sucrose, 10 mM MES, pH 7.4, 1 mM EGTA and 0.1 mM PMSF and rehomogenized and centrifuged as above. After discarding the pellet, the supernatant was incubated with 1% (w/v) N-laurylsarcosine ionic detergent for 1 h at room

temperature on an orbital shaker. The mixture was then centrifuged (87,000 × *g*, 35 min), and the supernatant was discarded. The pellet was resuspended in 10 mM MES, pH 7.0 (0.2 mL/g tissue), then layered onto a discontinuous sucrose gradient constructed from layers of 1 M, 1.5 M, and 2 M sucrose prepared in 10 mM MES, pH 7.0. After centrifugation (112,000 × *g*, 2.4 h), fractions were removed from the top and examined by TEM. The 1 M sucrose layer and the 1 M/1.5 M sucrose interface contained the majority of tau filaments and were stored in aliquots at 80°C until used.

To solubilize filaments, sucrose gradient fractions were incubated (1 h at 37°C) in 2 M guanidinium thiocyanate, then centrifuged at 100,000 × *g* (40 min at 4°C). The resulting supernatants were dialyzed (four changes over 30 h at 4°C) in 25 mM ammonium acetate, pH 7.4, then centrifuged (100,000 × *g*, 40 min at 4°C) to yield soluble PHF-tau. Samples were then dried under vacuum and stored at −20°C until used.

T-REx-293-derived tau protein

Stable tetracycline-inducible human 2N4R cells (T-REx-293 tau cells) prepared as described previously [29] were grown (37°C with 5% CO_2) in Dulbecco's modified Eagle's medium (DMEM) supplemented with 10% fetal bovine serum, 100 U/ml penicillin G, 250 ng/ml amphotericin B, 100 μg/ml streptomycin and 5 μg/ml blasticidin S. To induce tau expression, cells were treated with tetracycline (500 ng/mL final concentration) for five days. To isolate soluble tau protein, T-REx-293 tau cells were homogenized in five volumes of homogenization buffer containing phosphoprotein phosphatase inhibitors plus 100 nM okadaic acid using a Teflon-glass homogenizer (10 strokes at 1000 RPM), then centrifuged (27,000 × *g*, 20 min at 4°C). The resulting supernatant was brought to 0.5 M NaCl and 2% 2-mercaptoethanol, boiled for 10 min, then centrifuged (27,000 × *g*, 20 min at 4°C) to yield a heat-stable supernatant. Perchloric acid was then added drop-wise at 4°C with stirring to 2.5% (w/v) final concentration. After isolating the acid-soluble fraction by centrifugation (27,000 × *g*, 20 min at 4°C), protein was concentrated by TCA precipitation (20% w/v) followed by two washes with cold acetone. Dry protein pellets were stored at −20°C until used. For subsequent analyses, TCA-precipitates were dissolved in 10 mM HEPES pH 7.4, 50 mM NaCl, 0.02% Brij-35.

SDS-PAGE and immunoblots

Tau proteins were separated on 8% acrylamide gels under conditions where all six human isoforms could be resolved. For direct visualization of tau protein, gels were stained with Coomassie blue or with silver using the SilverQuest silver staining kit (Thermo-Fisher, LC6070) following the basic staining protocol outlined in manufacturer's instructions. For detection of tau immunoreactivity, gel contents were transferred to polyvinylidene fluoride or nitrocellulose membranes as described previously [30, 31] which were then probed using Tau5 as primary antibody (2N4R epitope Ser^{210}-Arg^{230}, [32, 33]). Immunoreactivity detected with horseradish peroxidase-labeled goat anti-mouse IgG (Thermo-Fisher, G-21040) and Pierce ECL Western Blotting Substrate (Thermo-Fisher, 32109) was captured on film. Electrophoretic migration was calibrated relative to a ladder of recombinant human tau isoforms (rPeptide, T-1007–1).

Proteomic analysis

Human brain-derived tau proteins were excised from Coomassie blue stained SDS-PAGE gels, trypsinized and the resulting peptides subjected to liquid chromatography–tandem mass spectrometry (LC-MS/MS) on a hybrid linear ion trap-Orbitrap mass spectrometer (LTQ-Orbitrap, Thermo Scientific) as described previously [24]. Mass spectra were searched against a manually curated database containing all known central nervous system isoforms of human tau using both MASCOT and Bioworks 3.3.1 SP1 with SEQUEST algorithms. Search parameters [34] included 20 ppm peptide mass tolerance, 1.0 amu fragment tolerance, static modification Cys + 57.02146 (carbamidomethylation) and variable modifications: Met +15.99491 (oxidation); Lys +14.01565 (monomethylation); Lys +28.03130 (dimethylation); Lys +42.04695 (trimethylation); Lys +42.01056 (acetylation); and Ser/Thr +79.96632 (phosphorylation) and −18.01054 (corresponding to β-elimination of phospho-Ser and phospho-Thr to dehydroalanine and dehydrobutyrine, respectively). Tryptic peptides with up to three missed cleavages, charge-state dependent cross correlation (XCorr) scores ≥ 1.5, 2.5, and 3.0 for 1+, 2+, and 3+ peptides, respectively, and delta correlation (ΔCn) > 0.1 were considered initial positive identifications. All MS/MS and spectra of identified post-translationally modified peptides from the initial screening were subjected to location probability analysis and manual verification. For MASCOT search results, modified peptides with initial MSCORE >20 were retained and validated by manual inspection. Only cases with ≥50% sequence coverage were included in proteomic analyses reported in Tables 1 and 2, and Figs. 1 and 2.

Targeted metabolomics analysis

SDS-PAGE fractionated, membrane-bound tau proteins were excised, hydrolyzed in HCl, and the resulting amino acid products subjected to LC-MS/MS on Sciex QTRAP 6500 triple-quadrupole mass spectrometer using the transitions and instrument settings described previously [31]. Spectra were acquired using turbo spray ionization at 2.5 kV in positive ion mode under control of Analyst 1.7 software. The relative proportion ((P_{K_X})) of all peptidyl-Lys residues in the form of N^{ε}-(methyl)-, N^{ε}-(dimethyl)-, or N^{ε}-(trimethyl)-L-lysine (1meK, 2meK, and 3meK, respectively) was calculated ratiometrically from mol amounts of all methyl-Lys species (*XmeK*) by the equation:

$$P_{K_X} = \frac{XmeK}{Lys + \sum_{X=1}^{3} XmeK} \quad (1)$$

The stoichiometry of total peptidyl-Lys methylation (*i.e.*, mol methyl groups per mol protein; S_K) was then calculated by summing the relative proportion of each methyl-Lys species and multiplying it by the number of peptidyl-Lys residues (N) expressed in human tau:

$$S_K = N \sum_{X=1}^{3} XP_{K_X} \quad (2)$$

This calculation assumed $N \approx 40.2$ mol Lys/mol tau protein, which represents an average value for all isoforms on the basis of their reported ratios in human brain [35].

Similarly, the relative proportion ((P_{R_X})) of all peptidyl-Arg residues in the form of N^G-methyl-L-arginine (1meR) or total symmetrical- (N^G,N^G) and nonsymmetrical- (N^G,$N^{G\prime}$) dimethyl-Larginine (2meR) was calculated ratiometrically from mol amounts of all methyl-Arg species (*XmeR*) by the equation:

$$P_{R_X} = \frac{XmeR}{Arg + \sum_{X=1}^{2} XmeR} \quad (3)$$

The stoichiometry of peptidyl-Arg methylation (*i.e.*, mol methyl groups per mol protein) was calculated by summing the relative proportion of each methyl-Arg species and multiplying it by the number of peptidyl-Arg residues (*N*) expressed in human tau:

$$S_R = N \sum_{X=1}^{2} XP_{R_X} \quad (4)$$

This calculation assumed $N = 14$ mol Arg/mol tau, which is shared by all human brain isoforms [36].

Statistical methods

Differences among methylation stoichiometries were analyzed by one-way ANOVA and Tukey's post hoc multiple comparison test using JMP 14.0 software (SAS Institute, Cary, NC). The null hypothesis was rejected at $p < 0.05$.

Results

Tau post-translational modifications in cognitively normal elderly human brain

To capture the effects of aging on tau PTMs, soluble tau protein was isolated and purified from post-mortem brains of cognitively normal elderly humans. The total cohort, which averaged age 84 ± 3 yrs, originated from three independent brain banks, spanned three neocortical regions, and met behavioral and pathological criteria to serve as non-demented controls (Table 1). Isolated human tau preparations from six cases were then digested with trypsin, and the resulting peptide fragments characterized by LC-MS/MS. Relative to 2N4R tau (the longest isoform in human brain), overall sequence coverage using this approach exceeded 84% of all amino acid residues, 87% of all Ser/Thr residues, and 84% of all Lys residues (Fig. 1A).

To identify phosphorylation sites, search parameters for phospho-peptide adducts as well as peptides containing the products of pSer and pThr β-elimination (dehydroalanine and dehydrobutyrine, respectively) were employed. As a result, peptides containing 31phosphorylation sites were found within the coverage area (Tables 2 and 3). When viewed within the context of 2N4R tau, phosphorylation sites localized with greatest frequency

within the projection and assembly domains outside the microtubule binding region (MTBR) (Fig. 1B). Identification of phospho-sites varied among cases, but pT181 and pT231 were replicated in all of them (Fig. 1B). These data confirmed that elderly brain-derived tau protein samples were extensively modified, and that our methods were adequate for detecting tau modifications with high mass accuracy.

We next searched for Lys modifications by setting search parameters for Lys acetylation, methylation, and ubiquitylation. Peptides containing each of the three modifications were found (Table 3), but unlike phosphorylation sites, they were observed in fewer numbers and with less replication consistency than phosphorylation sites in this cohort. (Fig. 1B). For example, acetylation at Lys24 was found in just one case, and three out of four detected ubiquitylation sites were found in only one case each (Fig. 1AB). In contrast, Lys methylation appeared at six sites, with five of these corresponding to 1meK (Fig. 1AB). Nonetheless, only monomethylation at K259 was robust, being observed in four out of six cases. Overall, monomethylation was the foremost Lys modification in this cohort.

Tau methylation changes with aging and disease

To estimate the effects of aging on tau PTM, the site distribution deduced for cognitively normal elderly cases was compared to the patterns we reported previously from a cognitively normal middle age cohort (mean age 55 ± 1 yr) analyzed under identical conditions and with similar overall sequence coverage [24]. With respect to phosphorylation, 22 of the 31 sites identified in elderly samples were shared between cohorts, with eight sites being unique to the elderly (Fig. 2A). Six of these (pT52, pT69, pT135, pS137, pT220 and pS324) were low replication consistency sites, being observed in just one case each (Fig. 1B). In contrast, pT123 and pS184 were found in at least two cases each, and may represent a more reliable index of age-related change in phosphorylation state. Unlike phosphorylation, Lys methylation was more heterogeneous, with modification of only K259, K267 and K290 being shared between the two cohorts. In addition, the elderly cohort contained fewer dimethylation sites relative to the middle age cohort (Fig. 2A). These data indicate that Lys methylation patterns differed qualitatively with normal aging.

The PTM pattern of the cognitively normal elderly cohort also was compared to the reported distributions of Ser/Thr phosphorylation (reviewed in [12]) and Lys methylation [25] in PHF-tau. The phosphorylation patterns overlapped substantially, with 20 of the 31 sites identified in elderly samples shared with PHF-tau, and with ten sites being unique to the elderly (Fig. 2B). However, seven of these sites (pT52, pT135, pS137, pT220, pT263, pS285 and pS324) were observed in just one case each. Conversely, PHF-tau reportedly contains many sites that were not present in soluble tau isolated from cognitively normal individuals (Fig. 2B). These results were consistent with previous comparisons between soluble tau from cognitively normal cases and PHF-tau from AD (reviewed in [12]). With respect to Lys methylation, both soluble cognitively normal elderly tau and PHF-tau were dominated by monomethylation, with site overlap limited to K267 and K290 (Fig. 2B). These two sites also were occupied in the cognitively normal middle age cohort, making them the only methylation sites shared among all three cohorts investigated (Fig. 2AB). Overall, proteomic analysis of human tau proteins identified Lys methylation as present in all cohorts, but with

low consistency among cases relative to phosphorylation, and with substantial variability among cohorts.

Tau methylation occurs at low stoichiometry

The biological impact of PTMs depends not only on the location of their sites, but also on site occupancy. To quantify overall site occupancy, the mol/mol stoichiometry of Lys methylation was determined ratiometrically on tissue-derived tau samples using a targeted metabolomics approach [31]. Tau samples were first vetted by SDS-PAGE (*i.e.*, under conditions that resolved all six isoforms) to assess whether they were of sufficient purity for this approach. When immunoblotted with monoclonal antibody Tau5, soluble tau from cognitively normal middle age and elderly cases electrophoresed with similar relative mobility as recombinant human tau isoform standards (Fig. 3AC). On the basis of silver staining, tau immunoreactive species represented the major proteins in the preparations (Fig. 3BD). In contrast, PHF-tau immunoreactivity prepared from the AD cases migrated more slowly on SDS-PAGE (Fig. 3E), consistent with established behavior (reviewed in [37]). Nonetheless, silver staining confirmed that the tau-immunoreactive species were the principal proteins present in these samples as well (Fig. 3F). Together these data show that brainderived tau proteins were prepared at adequate levels of purity for ratiometric analysis [31].

Tissue-derived tau samples were then SDS-PAGE purified, hydrolyzed to individual amino acids in HCl, then assayed for 1meK, 2meK and 3meK by LC-MS/MS [31]. The highest stoichiometries of Lys methylation were found in soluble tau from cognitively normal middle age cases, where 1meK, 2meK and 3meK all reached statistical significance (Fig. 4ABC). Total stoichiometry attained ~0.6 mol methylated residue/mol tau, or ~1 mol methyl group/mol tau protein in this cohort. In contrast, only 1meK could be quantified in soluble tau from the cognitively normal elderly cohort, where it attained a stoichiometry of ~0.2 mol 1meK/mol tau (Fig. 4ABC). PHF-tau from the AD cohort failed to reach statistical significance for any methylLys form (Fig 4ABC). These results reveal that while detectable by LC-MS/MS methods, the bulk levels of methyl-Lys do not rise to the levels reported to be associated with depression of tau aggregation propensity [24].

In addition to methyl-Lys, soluble tau isolated from mouse brain reportedly contains methyl-Arg residues [38]. To determine whether this modification also resided in human tau, samples from all three human cohorts were subjected to targeted metabolomics analysis programmed to detect methyl-Arg. Like methyl-Lys, both N^G-methyl-L-arginine (1meR) and N^G,N^G- and N^G,$N^{G'}$-dimethyl-L-arginine (2meR) are stable to acid hydrolysis and are detectable by LC/MS-MS [31]. Results showed that stoichiometries of 1meR (Fig. 4D) and 2meR (Fig. 4E) achieved statistical significance in all cohorts ($p < 0.05$), but at low stoichiometries (*i.e.*, <0.1 mol methylated Arg residue/mol tau protein). These data indicate that Arg methylation, while detectable, is a very low stoichiometry modification in post-mortem human brain neocortex.

3.4. Tau methylation can be modeled in cell culture

To determine whether tau methylation could be recapitulated in cultured cells, T-Rex-293 tau cells stably transfected with human 2N4R tau were investigated. Unlike wild-type HEK293 cells, stable T-Rex-293 tau cells support high-level and inducible expression of tau [29]. On the basis of SDS-PAGE analysis, 2N4R tau isolated from these cells was of sufficient purity for LC-MS/MS analysis (Fig. 5A). Results showed that 1meK and 2meK stoichiometries reached statistical significance, with monomethylation being the predominant modification in these cells (Fig. 5B). Altogether, Lys methylation reached ~0.1 mol methylated residue/mol 2N4R tau in these cells. In contrast, only trace levels of Arg methylation were detected, which reached statistical significance solely for 2meR (Fig 5B). These data indicate that tau stable T-Rex-293 cells can recapitulate human tau methylation signature in an experimentally tractable human cell culture system under basal conditions.

Discussion

These data extend direct mass spectrometry-based detection of tau PTM to a human cohort composed of cognitively normal elderly individuals. Together with previously reported results from cognitively normal middle age and AD cohorts [24, 25], the data resolve several issues associated with Lys modification. First, Lys methylation was detected in all investigated cohorts, indicating that it is a physiological tau modification. Monomethylation of K259 was the most consistently observed product *within* the cognitively normal middle age and elderly cohorts, whereas mono- or dimethylation of K267 was the most consistently observed product *among* all cohorts. Both K259 and K267 reside in a segment of the MTBR that mediates association between recombinant non-modified tau and microtubules [39] and that lies adjacent to the core region of AD-derived tau filaments [40]. Because this segment was not resolved in structural studies of ADderived filaments [41, 42], atomic resolution images of these sites in aggregates currently are unavailable (although electron density consistent with K331 methylation was observed in AD-derived tau aggregates [42], peptides containing this residue were not captured in proteomics experiments [25]). Sites other than K259 or K267 were observed inconsistently within cohorts, suggesting that they reflected low occupancy or stochastic modifications. Nonetheless, the predominant form of methylation was consistent within cohorts, with dimethylated peptides predominating in cognitively normal middle age relative to elderly cases (and not detectable in AD-aggregate tau). Together these data indicate that Lys methylation status differs qualitatively with aging and disease. As established for tau phosphorylation, however, biological impact of tau PTM also depends on stoichiometry. Here bulk tau methylation stoichiometry was captured using targeted metabolomics methods [31]. Unlike other ratiometric methods that leverage proteomic (*e.g.*, FLEXITau, [43]) or immunological technique [44], this approach is not influenced by neighboring PTMs that can complicate quantification and render it context dependent. Our quantification data confirmed that tau methylation shifted from predominantly 2meK to 1meK with aging and disease. However, they also revealed that bulk stoichiometries of methyl-Lys never rose above ~1 mol methyl group/mol tau in any cohort. This is well below the levels required to depress tau aggregation propensity *in vitro* [24]. We conclude that methylation levels are probably too low to depress tau aggregation propensity under normal physiological conditions.

What then is the significance of tau methylation? One potential application is as a biomarker of tau modification state, which in addition to changes in phosphorylation state shifts from predominantly 2meK to 1meK with aging and disease. However, as shown herein, bulk tau methylation stoichiometries are low, and fragmentation of tau in cerebrospinal fluid [45, 46] likely lowers detectable levels still further. As a result, utility will likely require detection sensitivities beyond the low fmol limit of quantification that targeted metabolomics methods currently deliver [31]). Another potential application is to protect tau against aggregation in disease by artificially raising its methylation levels. This could be achieved through pharmacological inhibition of tau demethylases. Indeed, other demethylases are established targets of AD drug discovery efforts [47]. However, neither the methyltransferases nor demethylases that act on tau protein are known. Here we showed that tau stable T-Rex-293 cells could recapitulate the Lys methylation pattern seen in human brain. These cells may offer a route for identifying tau modification enzymes and for determining which demethylases may be drug discovery targets.

A second finding regarding Lys modification concerned acetylation, which we found on K44 in a single cognitively normal elderly case. It joins K174 and K281 as the third acetylation site identified by proteomics methods. However, we found that K44 acetylation had low replication consistency among cases. Because most mammalian Lys acetylation occurs at low stoichiometry *in vivo* [48, 49], it will be important to establish whether the absolute stoichiometry of tau acetylation is significant in human cases.

Third, we identified four Lys ubiquitylation sites in the cognitively normal elderly cohort, two of which (K180 and K280) were novel. This brings the number of reported tau ubiquitylation sites to 19 (out of ~40 possible Lys residues in all tau isoforms), with the majority positioned in the MTBR where they overlap with methylation sites (reviewed in [15]). All sites identified herein displayed low replication consistency, which is in accordance with the transient and reversible nature of ubiquitylation. Overall, the data point toward tau ubiquitylation having limited site specificity.

Limitations

The analysis described herein assumes that Lys post-translational modifications survived through post mortem interval and laboratory purification. Although effort was made to control the latter through inclusion of phosphoprotein phosphatase, deacetylase and protease inhibitors, no inhibitors for putative tau demethylases were available. More importantly, no treatment could ameliorate the effects of post-mortem interval, which at a minimum can alter tau phosphorylation patterns [50]. For example, biopsy-derived human tau protein migrates with marked band shifts on SDS-PAGE [35, 51] whereas post-mortem tau migrates more closely with non-phospho tau [51]. Similar relative mobilities were found herein (Fig. 3AB). Nonetheless, 31 phosphorylation sites were detected in the cognitively normal elderly cohort, some with replication consistencies exceeding those observed for any Lys modification. Although most phosphorylation sites overlapped with those identified previously in a cognitively normal middle age cohort, some including newly identified T127 [52] were unique to the elderly population. This site, which also is occupied in AD brain [52], may provide another PTM biomarker of aging and disease.

In summary, we have demonstrated that soluble tau isolated from cognitively normal elderly individuals is methylated on Lys residues. Methylation site distribution changes with aging and disease, but overall stoichiometry is low relative to phosphorylation. Recapitulation of tau methylation pattern in tau stable T-Rex-293 cells suggests a path forward for identifying tau methyltransferases/demethylases and interrogating their function in biological model systems.

Acknowledgments

We thank Dr. Douglas W. Scharre for access to the Buckeye Brain Bank and Dr. H. Ronald Zielke for access to the NICHD Brain and Tissue Bank for Developmental Disorders at the University of Maryland, Baltimore, MD (contract HHSN275200900011C, Ref. No. N01-HD-90011). We also acknowledge the BioAnalytical Facility at the University of North Texas for support of mass spectrometry analyses. This work was supported by grants from the Public Health Service (NS07741 and AG045018). C.N.H. was supported by Molecular Biophysics Training Grant T32 GM118291.

References

[1]. Spillantini MG, Goedert M (2013) Tau pathology and neurodegeneration. Lancet Neurol 12, 609–622. [PubMed: 23684085]

[2]. Wang Y, Mandelkow E (2016) Tau in physiology and pathology. Nat Rev Neurosci 17, 5–21. [PubMed: 26631930]

[3]. Morris M, Maeda S, Vossel K, Mucke L (2011) The many faces of tau. Neuron 70, 410–426. [PubMed: 21555069]

[4]. Ghoshal N, Garcia-Sierra F, Wuu J, Leurgans S, Bennett DA, Berry RW, Binder LI (2002) Tau conformational changes correspond to impairments of episodic memory in mild cognitive impairment and Alzheimer's disease. Exp Neurol 177, 475–493. [PubMed: 12429193]

[5]. Wu JW, Herman M, Liu L, Simoes S, Acker CM, Figueroa H, Steinberg JI, Margittai M, Kayed R, Zurzolo C, Di Paolo G, Duff KE (2013) Small misfolded Tau species are internalized via bulk endocytosis and anterogradely and retrogradely transported in neurons. J Biol Chem 288, 1856–1870. [PubMed: 23188818]

[6]. Mirbaha H, Holmes BB, Sanders DW, Bieschke J, Diamond MI (2015) Tau Trimers Are the Minimal Propagation Unit Spontaneously Internalized to Seed Intracellular Aggregation. J Biol Chem 290, 14893–14903. [PubMed: 25887395]

[7]. Bramblett GT, Trojanowski JQ, Lee VM (1992) Regions with abundant neurofibrillary pathology in human brain exhibit a selective reduction in levels of binding-competent tau and accumulation of abnormal tau-isoforms (A68 proteins). Lab Invest 66, 212–222. [PubMed: 1735956]

[8]. Biernat J, Gustke N, Drewes G, Mandelkow EM, Mandelkow E (1993) Phosphorylation of Ser262 strongly reduces binding of tau to microtubules: distinction between PHF-like immunoreactivity and microtubule binding. Neuron 11, 153–163. [PubMed: 8393323]

[9]. Huseby CJ, Bundschuh R, Kuret J (2019) The role of annealing and fragmentation in human tau aggregation dynamics. J Biol Chem 294, 4728–4737. [PubMed: 30745358]

[10]. Despres C, Byrne C, Qi H, Cantrelle FX, Huvent I, Chambraud B, Baulieu EE, Jacquot Y, Landrieu I, Lippens G, Smet-Nocca C (2017) Identification of the Tau phosphorylation pattern that drives its aggregation. Proc Natl Acad Sci U S A 114, 9080–9085. [PubMed: 28784767]

[11]. Alonso A, Zaidi T, Novak M, Grundke-Iqbal I, Iqbal K (2001) Hyperphosphorylation induces selfassembly of tau into tangles of paired helical filaments/straight filaments. Proc. Natl. Acad. Sci. U.S.A 98, 6923–6928. [PubMed: 11381127]

[12]. Simic G, Babic Leko M, Wray S, Harrington C, Delalle I, Jovanov-Milosevic N, Bazadona D, Buee L, de Silva R, Di Giovanni G, Wischik C, Hof PR (2016) Tau Protein Hyperphosphorylation and Aggregation in Alzheimer's Disease and Other Tauopathies, and Possible Neuroprotective Strategies. Biomolecules 6, 6. [PubMed: 26751493]

[13]. Hanger DP, Anderton BH, Noble W (2009) Tau phosphorylation: the therapeutic challenge for neurodegenerative disease. Trends Mol Med 15, 112–119. [PubMed: 19246243]

[14]. Wang JZ, Xia YY, Grundke-Iqbal I, Iqbal K (2013) Abnormal hyperphosphorylation of tau: sites, regulation, and molecular mechanism of neurofibrillary degeneration. J Alzheimers Dis 33 Suppl 1, S123–139. [PubMed: 22710920]

[15]. Kontaxi C, Piccardo P, Gill AC (2017) Lysine-Directed Post-translational Modifications of Tau Protein in Alzheimer's Disease and Related Tauopathies. Front Mol Biosci 4, 56. [PubMed: 28848737]

[16]. Dickey CA, Yue M, Lin WL, Dickson DW, Dunmore JH, Lee WC, Zehr C, West G, Cao S, Clark AM, Caldwell GA, Caldwell KA, Eckman C, Patterson C, Hutton M, Petrucelli L (2006) Deletion of the ubiquitin ligase CHIP leads to the accumulation, but not the aggregation, of both endogenous phospho- and caspase-3-cleaved tau species. J Neurosci 26, 6985–6896. [PubMed: 16807328]

[17]. Petrucelli L, Dickson D, Kehoe K, Taylor J, Snyder H, Grover A, De Lucia M, McGowan E, Lewis J, Prihar G, Kim J, Dillmann WH, Browne SE, Hall A, Voellmy R, Tsuboi Y, Dawson TM, Wolozin B, Hardy J, Hutton M (2004) CHIP and Hsp70 regulate tau ubiquitination, degradation and aggregation. Hum Mol Genet 13, 703–714. [PubMed: 14962978]

[18]. Cohen TJ, Guo JL, Hurtado DE, Kwong LK, Mills IP, Trojanowski JQ, Lee VM (2011) The acetylation of tau inhibits its function and promotes pathological tau aggregation. Nat Commun 2, 252. [PubMed: 21427723]

[19]. Min SW, Chen X, Tracy TE, Li Y, Zhou Y, Wang C, Shirakawa K, Minami SS, Defensor E, Mok SA, Sohn PD, Schilling B, Cong X, Ellerby L, Gibson BW, Johnson J, Krogan N, Shamloo M, Gestwicki J, Masliah E, Verdin E, Gan L (2015) Critical role of acetylation in tau-mediated neurodegeneration and cognitive deficits. Nat Med 21, 1154–1162. [PubMed: 26390242]

[20]. Irwin DJ, Cohen TJ, Grossman M, Arnold SE, McCarty-Wood E, Van Deerlin VM, Lee VM, Trojanowski JQ (2013) Acetylated tau neuropathology in sporadic and hereditary tauopathies. Am J Pathol 183, 344–351. [PubMed: 23885714]

[21]. Grinberg LT, Wang X, Wang C, Sohn PD, Theofilas P, Sidhu M, Arevalo JB, Heinsen H, Huang EJ, Rosen H, Miller BL, Gan L, Seeley WW (2013) Argyrophilic grain disease differs from other tauopathies by lacking tau acetylation. Acta Neuropathol 125, 581–593. [PubMed: 23371364]

[22]. Tracy TE, Sohn PD, Minami SS, Wang C, Min SW, Li Y, Zhou Y, Le D, Lo I, Ponnusamy R, Cong X, Schilling B, Ellerby LM, Huganir RL, Gan L (2016) Acetylated Tau Obstructs KIBRA-Mediated Signaling in Synaptic Plasticity and Promotes Tauopathy-Related Memory Loss. Neuron 90, 245260.

[23]. Min SW, Cho SH, Zhou Y, Schroeder S, Haroutunian V, Seeley WW, Huang EJ, Shen Y, Masliah E, Mukherjee C, Meyers D, Cole PA, Ott M, Gan L (2010) Acetylation of tau inhibits its degradation and contributes to tauopathy. Neuron 67, 953–966. [PubMed: 20869593]

[24]. Funk KE, Thomas SN, Schafer KN, Cooper GL, Liao Z, Clark DJ, Yang AJ, Kuret J (2014) Lysine methylation is an endogenous post-translational modification of tau protein in human brain and a modulator of aggregation propensity. Biochem J 462, 77–88. [PubMed: 24869773]

[25]. Thomas SN, Funk KE, Wan Y, Liao Z, Davies P, Kuret J, Yang AJ (2012) Dual modification of Alzheimer's disease PHF-tau protein by lysine methylation and ubiquitylation: a mass spectrometry approach. Acta Neuropathol 123, 105–117. [PubMed: 22033876]

[26]. Ksiezak-Reding H, Liu WK, Yen SH (1992) Phosphate analysis and dephosphorylation of modified tau associated with paired helical filaments. Brain Res 597, 209–219. [PubMed: 1472994]

[27]. Greenberg SG, Davies P (1990) A preparation of Alzheimer paired helical filaments that displays distinct tau proteins by polyacrylamide gel electrophoresis. Proc Natl Acad Sci U S A 87, 5827–5831. [PubMed: 2116006]

[28]. Ksiezak-Reding H, Wall JS (1994) Mass and physical dimensions of two distinct populations of paired helical filaments. Neurobiol Aging 15, 11–19. [PubMed: 8159256]

[29]. Bandyopadhyay B, Li G, Yin H, Kuret J (2007) Tau aggregation and toxicity in a cell culture model of tauopathy. J Biol Chem 282, 16454-16464.

[30]. Li G, Yin H, Kuret J (2004) Casein kinase 1 delta phosphorylates Tau and disrupts its binding to microtubules. J Biol Chem 279, 15938-15945.

[31]. Cooper GL, Huseby CJ, Chandler CN, Cocuron JC, Alonso AP, Kuret J (2018) A liquid chromatography tandem mass spectroscopy approach for quantification of protein methylation stoichiometry. Anal Biochem 545, 72–77. [PubMed: 29407179]

[32]. LoPresti P, Szuchet S, Papasozomenos SC, Zinkowski RP, Binder LI (1995) Functional implications for the microtubule-associated protein tau: localization in oligodendrocytes. Proc Natl Acad Sci U S A 92, 10369–10373. [PubMed: 7479786]

[33]. Carmel G, Mager EM, Binder LI, Kuret J (1996) The structural basis of monoclonal antibody Alz50's selectivity for Alzheimer's disease pathology. J Biol Chem 271, 32789-32795.

[34]. Thomas SN, Yang AJ (2017) Mass Spectrometry Analysis of Lysine Posttranslational Modifications of Tau Protein from Alzheimer's Disease Brain. Methods Mol Biol 1523, 161–177. [PubMed: 27975250]

[35]. Hong M, Zhukareva V, Vogelsberg-Ragaglia V, Wszolek Z, Reed L, Miller BI, Geschwind DH, Bird TD, McKeel D, Goate A, Morris JC, Wilhelmsen KC, Schellenberg GD, Trojanowski JQ, Lee VM (1998) Mutation-specific functional impairments in distinct tau isoforms of hereditary FTDP-17. Science 282, 1914–1917. [PubMed: 9836646]

[36]. Goedert M, Jakes R (1990) Expression of separate isoforms of human tau protein: correlation with the tau pattern in brain and effects on tubulin polymerization. EMBO J 9, 4225–4230. [PubMed: 2124967]

[37]. Lee VM, Goedert M, Trojanowski JQ (2001) Neurodegenerative tauopathies. Annu Rev Neurosci 24, 1121–1159. [PubMed: 11520930]

[38]. Morris M, Knudsen GM, Maeda S, Trinidad JC, Ioanoviciu A, Burlingame AL, Mucke L (2015) Tau post-translational modifications in wild-type and human amyloid precursor protein transgenic mice. Nat Neurosci 18, 1183–1189. [PubMed: 26192747]

[39]. Kellogg EH, Hejab NMA, Poepsel S, Downing KH, DiMaio F, Nogales E (2018) Near-atomic model of microtubule-tau interactions. Science 360, 1242–1246. [PubMed: 29748322]

[40]. Novak M, Kabat J, Wischik CM (1993) Molecular characterization of the minimal protease resistant tau unit of the Alzheimer's disease paired helical filament. EMBO J 12, 365–370. [PubMed: 7679073]

[41]. Fitzpatrick AWP, Falcon B, He S, Murzin AG, Murshudov G, Garringer HJ, Crowther RA, Ghetti B, Goedert M, Scheres SHW (2017) Cryo-EM structures of tau filaments from Alzheimer's disease. Nature 547, 185–190. [PubMed: 28678775]

[42]. Falcon B, Zhang W, Schweighauser M, Murzin AG, Vidal R, Garringer HJ, Ghetti B, Scheres SHW, Goedert M (2018) Tau filaments from multiple cases of sporadic and inherited Alzheimer's disease adopt a common fold. Acta Neuropathol 136, 699–708. [PubMed: 30276465]

[43]. Mair W, Muntel J, Tepper K, Tang S, Biernat J, Seeley WW, Kosik KS, Mandelkow E, Steen H, Steen JA (2016) FLEXITau: Quantifying Post-translational Modifications of Tau Protein in Vitro and in Human Disease. Anal Chem 88, 3704–3714. [PubMed: 26877193]

[44]. Fuchs SM, Krajewski K, Baker RW, Miller VL, Strahl BD (2011) Influence of combinatorial histone modifications on antibody and effector protein recognition. Curr Biol 21, 53–58. [PubMed: 21167713]

[45]. Johnson GV, Seubert P, Cox TM, Motter R, Brown JP, Galasko D (1997) The tau protein in human cerebrospinal fluid in Alzheimer's disease consists of proteolytically derived fragments. J Neurochem 68, 430–433. [PubMed: 8978756]

[46]. Meredith JE Jr., Sankaranarayanan S, Guss V, Lanzetti AJ, Berisha F, Neely RJ, Slemmon JR, Portelius E, Zetterberg H, Blennow K, Soares H, Ahlijanian M, Albright CF (2013) Characterization of novel CSF Tau and ptau biomarkers for Alzheimer's disease. PLoS One 8, e76523.

[47]. Voronkov M, Braithwaite SP, Stock JB (2011) Phosphoprotein phosphatase 2A: a novel druggable target for Alzheimer's disease. Future Med Chem 3, 821–833. [PubMed: 21644827]

[48]. Tatham MH, Cole C, Scullion P, Wilkie R, Westwood NJ, Stark LA, Hay RT (2017) A Proteomic Approach to Analyze the Aspirin-mediated Lysine Acetylome. Mol Cell Proteomics 16, 310–326. [PubMed: 27913581]

[49]. Weinert BT, Moustafa T, Iesmantavicius V, Zechner R, Choudhary C (2015) Analysis of acetylation stoichiometry suggests that SIRT3 repairs nonenzymatic acetylation lesions. EMBO J 34, 2620–2632. [PubMed: 26358839]

[50]. Wang Y, Zhang Y, Hu W, Xie S, Gong CX, Iqbal K, Liu F (2015) Rapid alteration of protein phosphorylation during postmortem: implication in the study of protein phosphorylation. Sci Rep 5, 15709.

[51]. Matsuo ES, Shin RW, Billingsley ML, Van deVoorde A, O'Connor M, Trojanowski JQ, Lee VM (1994) Biopsy-derived adult human brain tau is phosphorylated at many of the same sites as Alzheimer's disease paired helical filament tau. Neuron 13, 989–1002. [PubMed: 7946342]

[52]. Giacomini C, Koo CY, Yankova N, Tavares IA, Wray S, Noble W, Hanger DP, Morris JDH (2018) A new TAO kinase inhibitor reduces tau phosphorylation at sites associated with neurodegeneration in human tauopathies. Acta Neuropathol Commun 6, 37. [PubMed: 29730992]

[53]. Goedert M, Spillantini MG, Potier MC, Ulrich J, Crowther RA (1989) Cloning and sequencing of the cDNA encoding an isoform of microtubule-associated protein tau containing four tandem repeats: differential expression of tau protein mRNAs in human brain. EMBO J 8, 393–399. [PubMed: 2498079]

[54]. von Bergen M, Friedhoff P, Biernat J, Heberle J, Mandelkow EM, Mandelkow E (2000) Assembly of tau protein into Alzheimer paired helical filaments depends on a local sequence motif (306VQIVYK311) forming β structure. Proc. Natl. Acad. Sci. U.S.A 97, 5129–5134. [PubMed: 10805776]

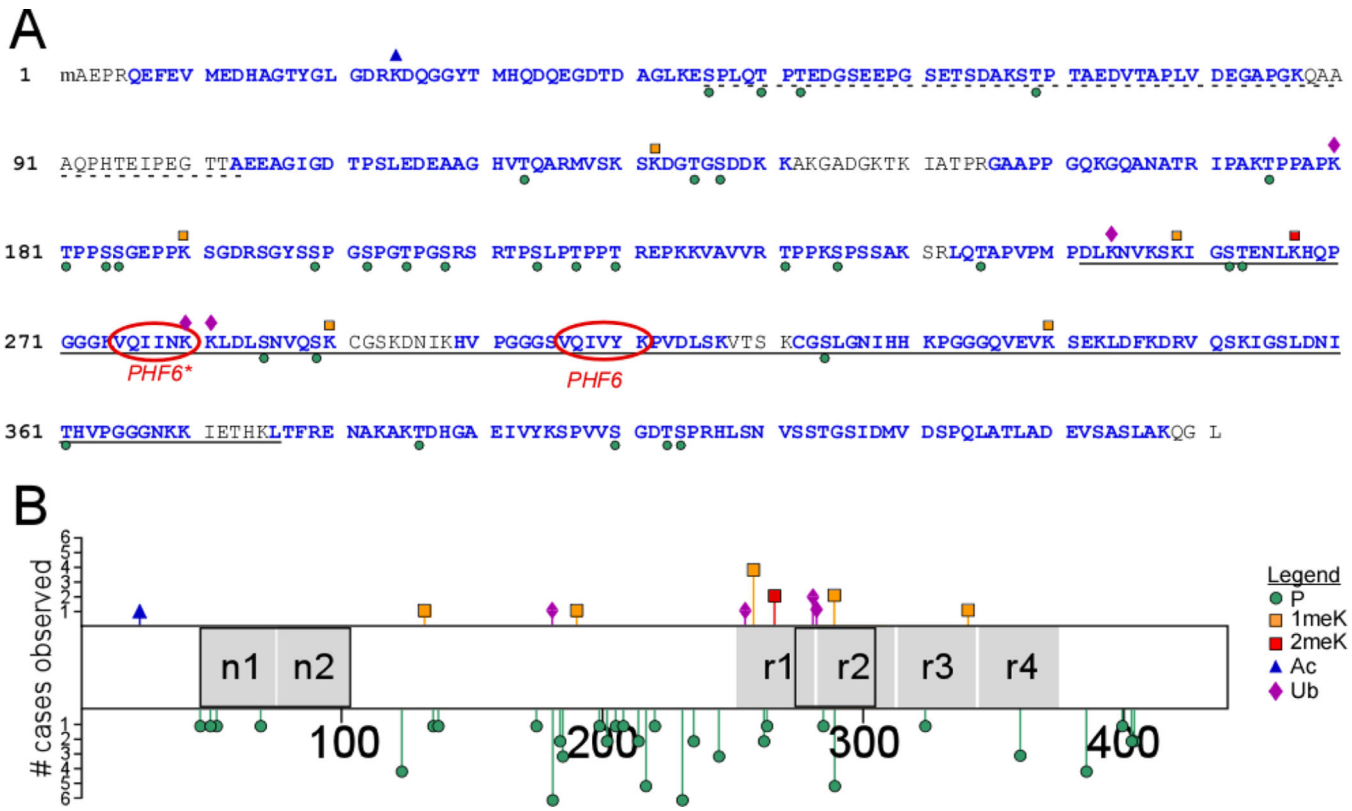

Fig. 1.

Post-translational modification sites on soluble tau proteins isolated from cognitively normal elderly identified by LC-MS/MS (cases 5, 6, 8–11, Table 1). (**A**) Identified tryptic peptides in the context of the human 2N4R isoform (NCBI accession number NP_005901), where the dotted underline depicts alternatively spliced projection domain segments n1 and n2, the solid underline identifies the MTBR (as defined in [53]), and PHF6/PHF6* mark the hexapeptide segments involved in filament nucleation [54]. Blue font color depicts sequence coverage. Phosphorylation (P) and ubiquitylation (Ub) sites are marked by green circles and purple diamonds, respectively, whereas mono- (1meK) and di-methylation (2meK) sites are indicated by orange and red squares, respectively. (**B**) Tau methylation and phosphorylation site distribution map (2N4R tau), showing location of modification sites relative to projection domain segments n1 and n2 and MTBR repeats r1 – r4 (black boxes depict alternatively spliced segments). The length of each bar corresponds to the number of cases in which the modification was found (# cases observed).

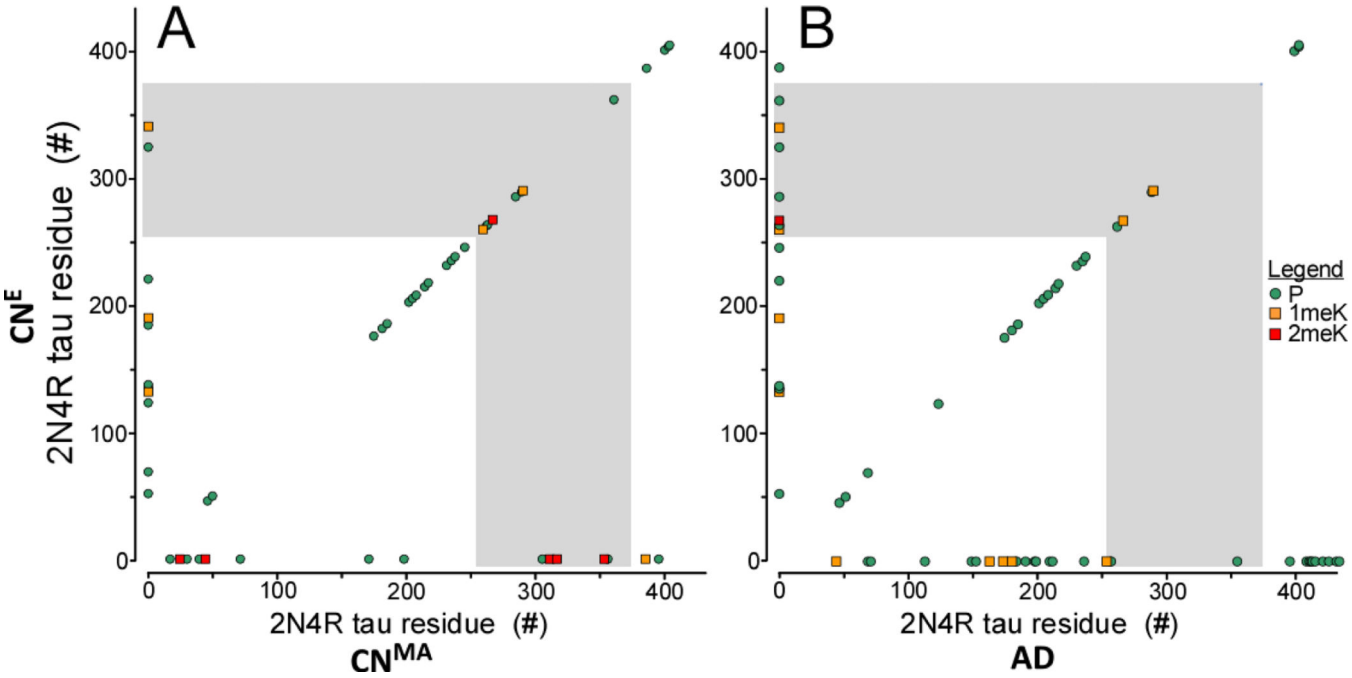

Fig. 2.

Modification sites in soluble tau protein isolated from cognitively normal elderly (CN^{E}) compared with (**A**) soluble tau from middle age (CN^{MA}) brain, and (**B**) PHF-tau from AD brain. Phosphorylation (P) are marked by green circles, whereas mono- (1meK) and di-methylation (2meK) sites are indicated by orange and red squares, respectively. The MTBR region is marked by gray shading. Symbols on the diagonal correspond to sites shared in between compared cohorts, whereas symbols located along the ordinate correspond to those found exclusively in the elderly relative to the compared cohort. In contrast, symbols located on the abscissa correspond to (**A**) sites found exclusively in the middle age cohort, and (**B**) sites found exclusively in PHF-tau relative to the cognitively normal elderly population.

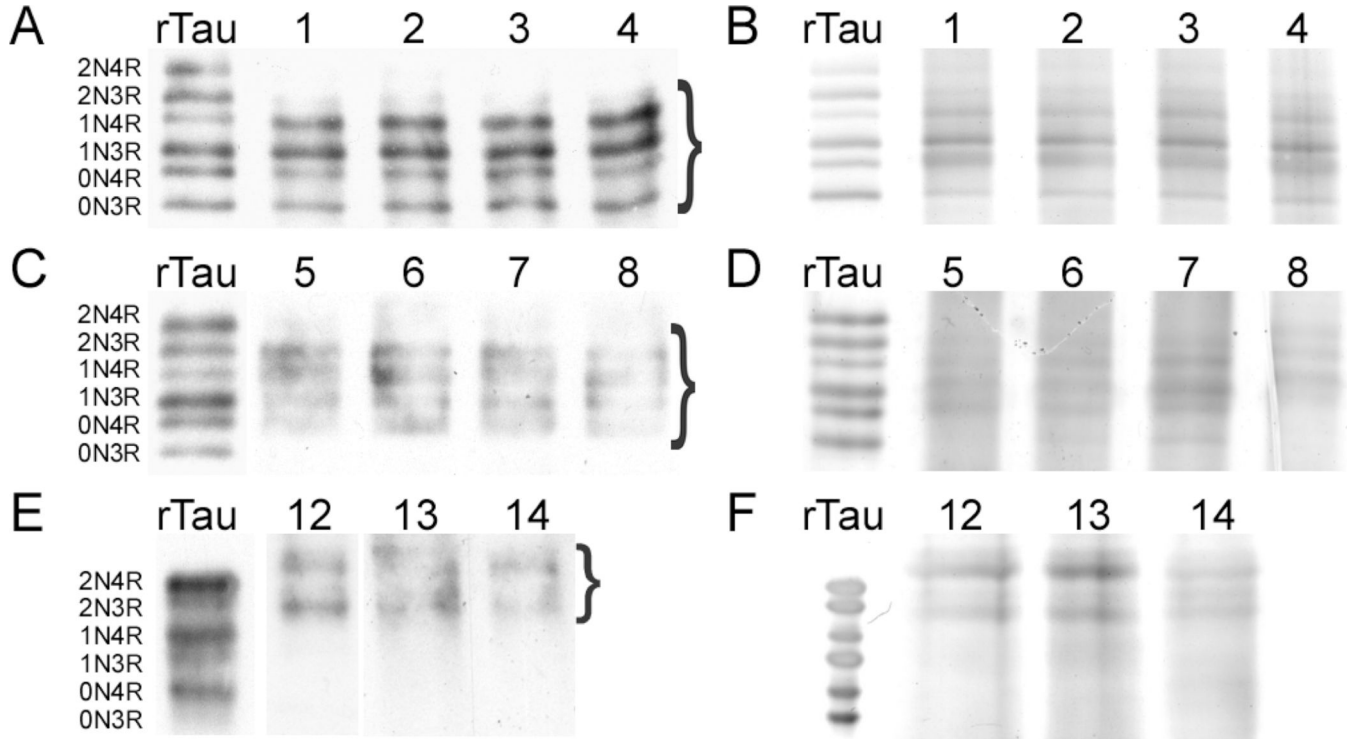

Fig. 3.

SDS-PAGE analysis of tau proteins isolated from cognitively normal middle age (**A,B**) cognitively normal elderly (**C,D**) and AD (**E,F**) brain samples. Lanes correspond to case numbers summarized in Table 1. Electrophoretic migration of all samples is shown relative to a ladder composed of all six human tau isoforms (rTau). (**A, C, E**) Gels were subjected to immunoblot analysis with monoclonal antibody Tau5. (**B, D, F**) Gels were stained with silver. Bands excised for targeted metabolomics analysis are marked by *brackets*.

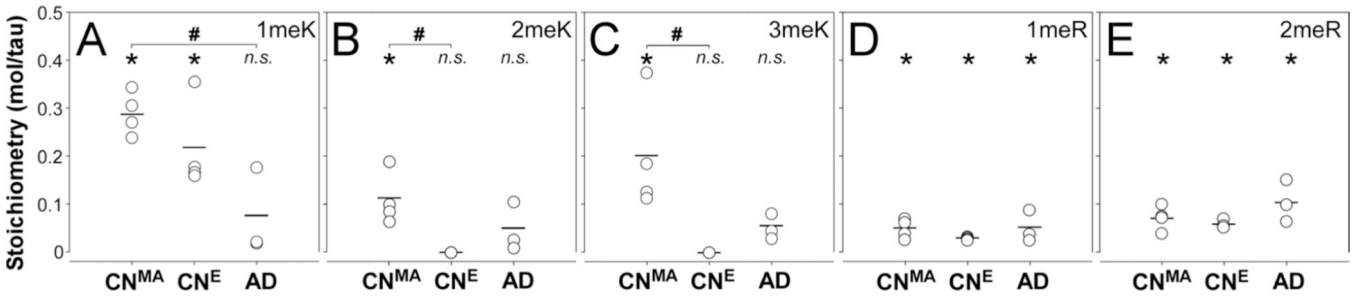

Fig. 4.

Methylation stoichiometries of soluble tau proteins purified from cognitively normal middle age (CN^{MA}) and elderly (CN^{E}) cases, and of aggregated tau from AD cases were determined by targeted metabolomics analysis. Each circular point represents methylation stoichiometry in a single biological replicate in units of mol residue/mol tau protein, whereas each bar represents the mean of all replicates. *, $p < 0.05$ compared to zero methylation stoichiometry, one-way ANOVA; #, $p < 0.05$ compared pairwise to all methyl-amino acid forms, ANOVA with Tukey's post hoc test; *n.s.*, not significant.

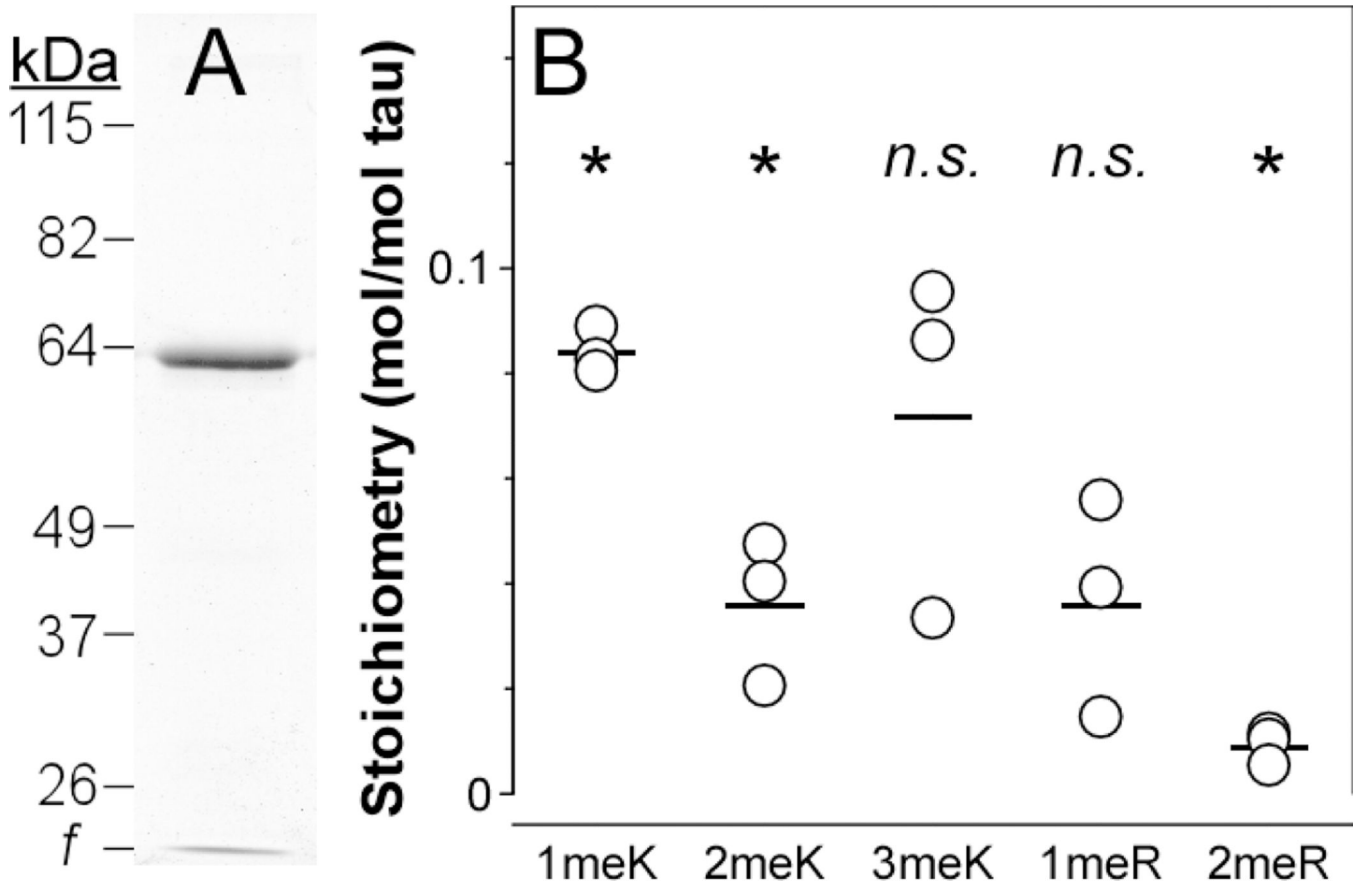

Fig. 5.

Methylation stoichiometries of soluble 2N4R tau isolated from T-Rex-293 tau cells determined by targeted metabolomics. **(A)** SDS-PAGE analysis (Coomassie blue stain; *f*, dye front). **(B)** Methylation stoichiometries for all analytes estimated by targeted metabolomics. Each circular point represents methylation stoichiometry in a single technical replicate in units of mol residue/mol tau protein, whereas each bar represents the mean of all replicates. *, $p < 0.05$ compared to zero methylation, one-way ANOVA; *n.s.*, not significant.

Table 1

Case demographics

Case (#)	Diag	Age (yr)	Sex	Race[a]	PMI[b] (h)	Source[c]	Identifier[d]	Comments[e]
1	Normal	55	M	AA	13	NICHD	5172	HASCVD; History of Diabetes, cocaine abuse, hypertension Acute Bronchopneumonia/ASCVD; Smoker, history of alcohol abuse, HASCVD; PTSS, No history of drug, alcohol abuse
2	Normal	57	M	C	5	NICHD	5117	
3	Normal	54	M	AA	10	NICHD	4923	
4	Normal	54	M	C	NA	OSU	116	NA
5	Normal	88	F	C	5.2	UCI	15–02	NFT/Aβ stage 2A; ApoE 3/3
6	Normal	86	M	C	2.9	UCI	24–11	NFT/Aβ stage 3A; ApoE 3/3
7	Normal	86	M	C	4.4	UCI	11–12	NFT/Aβ stage 2-; ApoE 3/3
8	Normal	83	M	C	1.8	UCI	25–01	NFT/Aβ stage 2-; ApoE 3/3
9	Normal	86	F	C	6.2	UCI	17–11	NFT/Aβ stage 3C; ApoE 3/3
10	Normal	81	M	C	17	NICHD	5352	Motor vehicle accident
11	Normal	80	M	C	10	NICHD	5444	Hypertensive cerebrovascular accident
12	AD	88	M	C	NA	OSU	394	NA
13	AD	81	F	C	NA	OSU	2571	NA
14	AD	63	M	C	NA	OSU	212	NA

[a] AA, African American; C, Caucasian.

[b] Post-mortem interval. NA, not available.

[c] NICHD, NICHD Brain and Tissue Bank for Developmental Disorders; UCI, University of California, Irvine; OSU, Ohio State University Buckeye Brain Bank

[d] Proteomic analysis of cases 1–4 was reported in [24].

[e] ASCVD, atherosclerotic cardiovascular disease; HASCVD, hypertensive arteriosclerotic cardiovascular disease; PTSS, Post Traumatic Stress Syndrome. NA, not available

Table 2

Ser/Thr modification sites identified on tau isolated from cognitively normal elderly human brains.

Trypsin digests of tissue-derived tau were analyzed by LC-MS/MS, and resulting *m/z* data were analyzed by MASCOT and SEQUEST using ±5 ppm mass tolerance.

aa residues[a]	Peptide[b]	Site	Mod[c]	SEQUEST		MASCOT	
				(ppm)	(XCorr)	(ppm)	(Score)
24–67	KDQGGYT**M**HQDQEGDTDAGLKE**S**PLQTPTED GSEEPGSETSDAK	M31/S46	Ox/DA			3.2	22.7
45–67	ESPLQ**T**PTEDGSEEPGSETSDAK	T50	P	4.56	2.82		
45–67	ESPLQTP**T**EDGSEEPGSETSDAK	T52	P			1.98	25.3
68–73; 103–126	S**T**PTAEAEEAGIGDTPSLEDEAAGHVTQAR	T69	DB			3.40	44.3
68–73; 103–126	STPTAEAEEAGIGDTPSLEDEAAGHV**T**QAR	T123	DB			3.74	21.1
131–143	SKDG**T**G**S**DDKKAK	T135/S137	P			−2.54	20.7
175–190	**T**PPAPKTPPSSGEPPK	T175	P	4.08	2.14		
175–190	TPPAPK**T**PPSSGEPPK	T181	P	2.43	2.88	0.36	23.5
175–190	TPPAPKTPP**S**SGEPPK	S184	P	4.60	2.77	−0.72	21.0
175–190	TPPAPKTPPS**S**GEPPK	S185	P	4.08	3.45	−1.32	34.3
195–209	SGYS**S**PGSPGTPGSR	S199	P			−0.68	59.2
195–209	SGYSSPG**S**PGTPGSR	S202	P	0.69	3.40	0.07	44.4
195–209	SGYSSPGSPG**T**PGSR	T205	P	0.19	2.56	−1.15	23.1
212–221	TP**S**LPTPPTR	S214	P	1.92	2.33	2.01	29.1
212–221	TPSLP**T**PPTR	T217	P	1.28	2.42		
212–221	TPSLPTPP**T**R	T220	P			1.31	21.9
225–234	KVAVVR**T**PPK	T231	P	2.33	2.29	−0.19	33.9
225–240	KVAVVRTPPK**S**PSSAK	S235	P			3.03	20.2
243–254	LQ**T**APVPMPDLK	T245	DB			2.79	23.6
260–267	IG**S**TENLK	S262	P	0.69	2.99	0.64	42.9
260–267	IGS**T**ENLK	T263	DB			−0.12	22.4
282–290	LDL**S**NVQSK	S285	DA			−1.21	25.2
282–290	LDLSNVQ**S**K	S289	DA	3.47	2.66	−0.10	38.3
322–340	CG**S**LGNIHHKPGGGQVEVK	S324	DA			1.64	23.0
354–369	IGSLDNI**T**HVPGGGNK	T361	DB	2.86	2.75	1.41	32.6

aa residues[a]	Peptide[b]	Site	Mod[c]	SEQUEST (ppm)	SEQUEST (XCorr)	MASCOT (ppm)	MASCOT (Score)
386–395	**T**DHGAEIVYK	T386	DB	1.89	2.76	−0.81	48.2
396–406	SPVV**S**GDTSPR	S400	P			−0.42	33.8
396–406	SPVVSGD**T**SPR	T403	P			0.34	57.5
396–406	SPVVSGDT**S**PR	S404	P	−0.86	2.55	−0.51	46.5

[a] Amino acid (aa) residue numbering conforms to human 2N4R tau.

[b] **S**, **T**, modified Ser or Thr residue, respectively; **M**, oxidized Met residue

[c] Modified residues (Mod) are DA, dehydroalanine; DB, dehydrobutyrine; Ox, Met-sulfoxide; P, phospho-Ser or phospho-Thr.

Table 3

Lys modification sites identified on soluble tau isolated from cognitively normal elderly human brains.

Trypsin digests of tissue-derived tau were analyzed by LC-MS/MS, and resulting *m/z* data were analyzed by MASCOT and SEQUEST using ±5 ppm mass tolerance as search parameter.

aa residues[a]	Peptide[b]	Site	Mod[c]	SEQUEST		MASCOT	
				(ppm)	(XCorr)	(ppm)	(Score)
	Acetylation						
24–44	**K**DQGGYTMHQDQEGDTDAGLK	K24	Ac	4.86	2.67		
	Methylation						
127–141	MVSKS**K**DGTGSDDKK	K132	1me			3.40	21.7
181–209	TPPSSGEPP**K**SGDRSGYSSPGSPG**T**PGSR	K190/T205	1me/P	-3.76	2.86		
181–209	TPPSSGEPP**K**SGDRSGYSSPGSPGTPG**S**R	K190/S208	1me/P	-3.76	2.53		
258–267	S**K**IGSTENLK	K259	1me	4.50	2.64	0.18	38.7
260–267	IGSTENL**K**	K267	2me			0.67	34.1
282–290	LDLSNVQS**K**	K290	1me	4.79	2.01	4.80	22.8
322–340	CGSLGNIHHKPGGGQVEV**K**	K340	1me			-3.00	23.3
	Ubiquitylation						
175–180	TPPAP**K**TPPSSGEPPK	K180	Ub	1.89	3.04		
243–257	LQTAPVP**M**PDL**K**NVK	K254	Ox/Ub	4.59	2.79		
275–280	VQIIN**K**K	K280	Ub			0.68	34.1
281–290	**K**LDLSNVQSK	K281	Ub	4.13	3.25	−0.31	22.6

[a] Amino acid (aa) residue numbering conforms to human 2N4R tau.

[b] **K**, modified Lys residues; **M**, oxidized Met residue

[c] Modified residues (Mod) are Ac, Ac-Lys; 1me, monomethyl-Lys; 2me, dimethyl-Lys; Ox, Met-sulfoxide; P, phospho-Ser or phospho-Thr; Ub, ubiquitylation